

Multicarrier Digital Pre-distortion/ Equalization Techniques for Non-linear Satellite Channels

R. Piazza¹ and M. R. Bhavani Shankar²
SnT, University of Luxembourg, Luxembourg, Luxembourg, L-1359

E. Zenteno³ and D. Rönnöw⁴
University of Gävle, Gävle, Sweden, 801-76

J. Grotz⁵ and F. Zimmer⁶
SES, Betzdorf, Luxembourg, 6815

M. Grasslin⁷ and F. Heckmann⁸
Steinbeis Transfer Centre for Space, Gäßfelden, Germany, 71126

and

S. Cioni⁹
ESA/ESTEC, Noordwijk, Netherlands, 2200 AG

Two key advances are envisaged for future missions: (a) spectrally efficient transmission to meet the increasing demand and (b) sharing of satellite capacity among different links to meet power/mass requirements. Joint amplification of multiple-carrier DVB-S2 signals using a single High-Power Amplifier (HPA) is a particular application of satellite resource sharing. However, effects specific to such a scenario that degrade power and spectral efficiencies include (a) an increased Adjacent Channel Interference caused by non-linear characteristic of the HPA and (b) increased peak to average power ratio. The paper studies signal processing techniques – digital pre-distortion (DPD) at the gateway and equalization (EQ) at the User Terminal – to mitigate the non-linear effects and improve power as well as spectral efficiencies. While the algorithms for DPD and EQ are described in literature, their use in multi-carrier scenario is novel and poses new challenges that are investigated in the paper

Nomenclature

<i>ACI</i>	=	Adjacent Channel Interferences
<i>ACM</i>	=	Adaptive Coding and Modulation
<i>APSK</i>	=	Amplitude Phase Shift Key
<i>BER</i>	=	Bit Error Rate
<i>DPD</i>	=	Digital PreDistortion
<i>DTH</i>	=	Direct To Home

¹ Doctoral Student, SnT, roberto.piazza@uni.lu, non-member

² Research Associate, SnT, Bhavani.Shankar@uni.lu, non-member

³ Doctoral Student, University of Gävle, Efrain.Zenteno@hig.se, non-member

⁴ Professor, University of Gävle, Daniel.Ronnöw@hig.se, non-member

⁵ Senior System Engineer, SES, Joel.Grotz@ses.com, non-member

⁶ Senior Manager, SES, Frank.Zimmer@ses.com, non-member

⁷ Senior Scientist, TZR, graesslin@tz-raumfahrt.de, non-member

⁸ PhD, TZR, heckmann@tz-raumfahrt.de, non-member

⁹ Communications Systems Engineer, TEC-ETC, stefano.cioni@esa.int, non-member

<i>EQ</i>	=	Equalization
<i>FIR</i>	=	Finite Impulse Response
<i>GW</i>	=	Gate Way
<i>HPA</i>	=	High Power Amplifier
<i>IBO</i>	=	Input Back-Off
<i>IMUX</i>	=	Input
<i>IRD</i>	=	Integrated Receiver Decoder
<i>ISI</i>	=	Inter-Symbol Interference
<i>L-TWTA</i>	=	Linearized Travelling Wave Tube Amplifier
<i>LS</i>	=	Least Squares
<i>OBO</i>	=	Output Back-Off
<i>OMUX</i>	=	Output
<i>SINR</i>	=	Signal to Interference plus Noise Ratio
<i>SNR</i>	=	Signal to Noise Ratio
<i>TWTA</i>	=	Travelling Wave Tube Amplifier

I. Introduction

In the arena of satellite communications, there is an increasing demand for higher data rates and bandwidth efficiency. A recent example of this trend is Viasat-1 that reaches a total throughput of 140 Gbps being the highest capacity broadcast satellite ever launched. In satellite broadcast systems, the data stream goes through the forward link, where we have, in general, three actors: the gateways, the satellite transponders and the end-receivers. The gateways collect the data and transmit the signal to one or more satellites. Each satellite transponder receives the data signal from one or more gateways and it then redirects it to the ground receivers. In widespread direct to home (DTH) services, the end receivers are fixed integrated receiver decoders (IRD) for mostly TV applications.

Transparent payloads, where the uplink data is mainly amplified and forwarded to users, are by far the most common telecom satellite architectures due to their competitive cost and technological flexibility since the signal processing carried out on the ground can be updated with the technological advancements in the course of the lifetime of the satellite. To ensure that the amplification is power-efficient, the High Power Amplifiers (HPA) are operated close to the saturation point. However, the on-board HPAs suffer from non-linear effects when driven close to saturation leading to undesired components being introduced into the signal of interest¹. High order signalling/modulation techniques, such as 16/32 amplitude and phase-shift keying modulation (APSK), are often used to increase spectral efficiency in DVB-S2 system². However, they are very sensitive to the non-linear distortions introduced by the on board HPA. This leads to a trade-off between power efficiency and signal degradation. Compensation techniques at the transmitter (known as pre-distortion) and at receiver (equalization) have been considered to mitigate the non-linear effects of the channel^{1, 3, 4}. Typical techniques include Look-up Tables¹ and Volterra functions for pre-distortion³ and Volterra equalizers for equalization⁴. An overview of these techniques is provided in Ref. 5.

The non-linear effects become even more prominent when multiple carriers are amplified using a single HPA. Such a situation arises very often, when different carriers share the same on-board HPA due to power/mass and flexibility requirements. This leads to spurious terms arising due to the inter-modulation products caused by the HPA non-linearity. A large guard-band between the carriers may be needed in order to avoid inter-modulation products or adjacent channel interference (ACI). Additionally, use of multiple carriers leads to the well-known high peak to average power ratios, and this increases the back-off used in the power amplification, leading to loss in amplification efficiency. These effects manifest as spectrum-inefficient frequency carrier segregation and power loss depending on the spectral efficiencies of the individual carriers. Apart from amplification, the payload forwards or channelizes the data from gateway to the respective users. This involves filtering causes inter symbol interference (ISI) which further degrades the performance. Compensation techniques for such a multi-carrier scenario are being only recently considered, for e. g., dual carrier predistortion^{6,7}, dual carrier Volterra equalizer⁸ and multiple carrier turbo-based equalizer⁹. However, the predistortion focuses on two carriers per HPA only and is described in a terrestrial system context. On the other hand, the equalization techniques, though considered for satellites, assume joint processing of all carriers at the receiver. This requirement may not always be feasible, especially when focussing on low complexity receivers. These motivate the study and design of pre-distortion and equalization techniques that can be applied to any number of carriers through a HPA, without the possibility of joint decoding. This paper is based on

the on-going European Space Agency ARTES 5 activity titled, “On Ground Multicarrier Digital Equalization/Predistortion Techniques for Single or Multi Gateway Applications”.

In the paper we describe: the scenario supporting multiple carriers per HPA, the non-linear channel model and its implications to multiple carrier transmissions in Section II, mitigation techniques in Section III and their performance analysis in Section IV. Conclusions are drawn in Section V.

II. Multiple Carrier Transmissions: Scenarios and Channel models

A. Scenarios

Recently launched wideband satellite transponders perform joint filtering and amplification of multiple carrier signals and the trend is envisaged for future systems as well. In such applications, different carriers are usually independent and dedicated to different user terminals or applications. Joint onboard filtering and amplification of the stream of carriers, allows significant saving in hardware complexity and weight.

Improved spectral and power efficiencies in this setting motivates the target scenario where a satellite broadcast transmission from a single gateway to many receivers with a transparent satellite transponder is considered. Each carrier channel is assumed to be compliant with DVB-S2 standard². Present multicarrier transponders have typical bandwidths of 33 and 72 MHz, carrier throughputs varying from 10MSps to 45 MSps and a linearized TWTA with typical OBO in the range of 2.9 – 4.5 dB.

From a system perspective, the predistortion needs to be designed under the assumption of a full knowledge of the channel characteristics in terms of filters, amplifiers etc at the gateway prior to launch, but no real time data on a loop back signal will be assumed available. Possible feedback from the receivers (dedicated receivers stations) can be considered available, at regular intervals, for channel reconfiguration. Concerning user terminals equalization, although the on-board joint amplification of multiple carriers can often occur, most of the current user receivers usually support demodulation and decoding only for a single carrier signal. The compensation of possible channel variations, e.g. TWTA parameters drift, will be delegated to the end receivers’ that have to track fast channel variations.

B. Non-Linear Satellite Channel Model

The typical model of the path between the transmitter and the receiver in a transparent satellite communication is shown in Figure 1. The signals from the GW are channelized to the satellite HPA through the IMUX filter whose amplitude and group delay response is depicted in

Figure 2. This wideband filter can be approximated as a linear system with memory (FIR filter) whose parameters are obtained from the response of

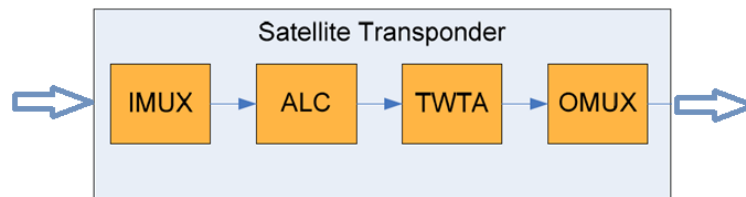


Figure 1: A typical Satellite Non-linear Channel

TWTAs constitute the commercially used onboard HPA and are intrinsically non-linear. Further, the TWTAs used in Ku-band can be assumed to have a transfer characteristic largely independent of the frequency. Such memoryless systems are characterized by the AM/AM and AM/ PM curves depicted in

Figure 3.

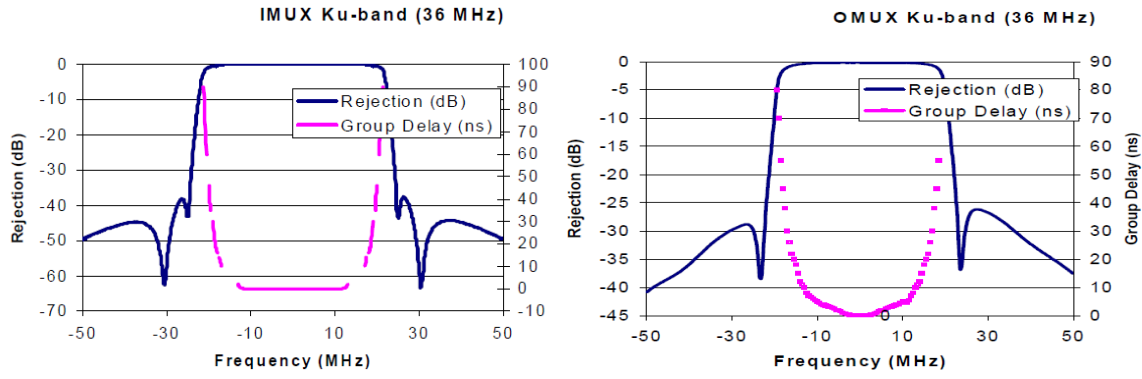


Figure 2: Ku band IMUX and OMUX filter characteristics

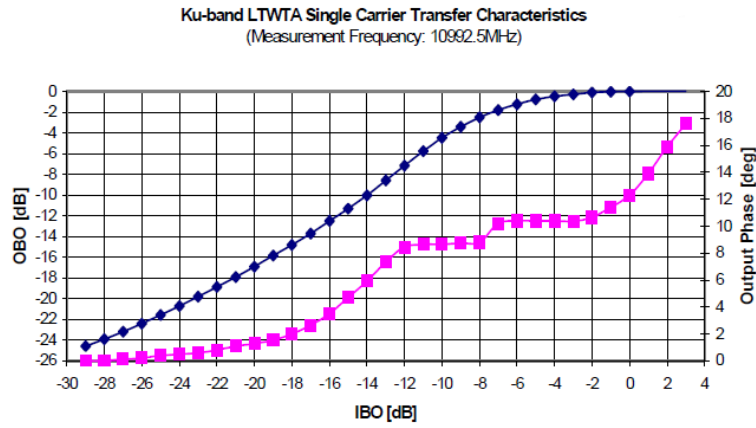


Figure 3: Ku band TWTA AM/AM and AM/PM characteristics

Essentially, the satellite channel can be abstracted as a non-linear system with memory. Such a channel leads to the following distortions:

- Constellation Warping caused by memoryless non-linearity
- Inter-Symbol Interference caused by
 - First order due to linear memory
 - Higher order due to non-linearity coupled with the filters
- Adjacent Channel interference due to non-linearity

These distortions are shown in Fig. 4, where in a three carrier system is simulated. Further, the distortions for a single carrier channel are also shown for reference.

C. Volterra Analysis

Being a nonlinear dynamic system, the satellite transponder is described by Volterra theory^{4, 10}, where complex baseband input signal, $x(n)$ and output signal, $y(n)$ are related as:

$$y(n) = \sum_{k=1}^{\infty} \sum_{n_1} \dots \sum_{n_k} h_k(n_1, n_2, \dots, n_k) \prod_{r=1}^p x(n - n_r) \prod_{q=p+1}^k x(n - n_q)^* \quad (1)$$

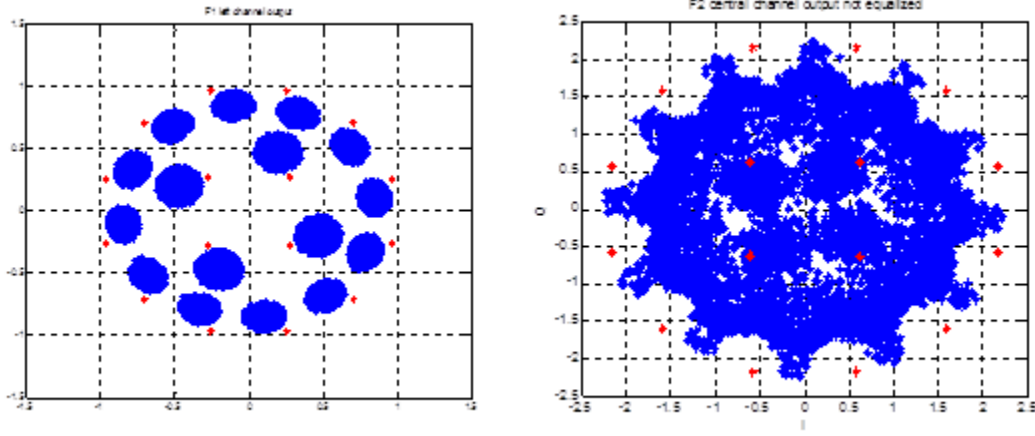


Figure 4: Scatter plot of received 16 APSK constellation: Single Carrier (left), Multicarrier Transmission (right)

where $h_k(n_1, n_2, \dots, n_k)$ are the Volterra kernels. Assuming M equi-spaced carriers (separation of Δf) with $s_m(n)$ denoting the baseband signal transmitted on the m^{th} carrier, we have,

$$x(n) = \sum_{m=0}^{M-1} s_m(n) e^{-j[2\pi m(\Delta f) + \phi_m]} \quad (2)$$

where ϕ_m is an arbitrary phase difference. Volterra series can be used to analyse the various distortions^{8,9} and Table 1 summarizes this analysis by presenting the different terms contributing to ISI and ACI for the case of three carriers (dependence on time index $-n-$ is dropped for ease of comprehension). For each carrier f_i all the third order in band interference terms satisfy the following condition:

$$\Delta f_i = \Delta f_{k_1} + \Delta f_{k_2} - \Delta f_{k_3} \quad (3)$$

where we have by the scenario $\Delta f_1 = \Delta f$, $\Delta f_2 = 0$ and $\Delta f_3 = -\Delta f$.

Table 1: Terms contributing to ICI and ACI for three carriers

Nonlinear order	Carrier #1	Carrier #2	Carrier #3	Bandwidth	Interference
1 st	s_1	s_2	s_3	Δf	ISI
3 rd	$s_1 s_1^* s_1$	$s_2 s_2^* s_2$	$s_3 s_3^* s_3$	$3\Delta f$	ISI+ACI
3 rd	$s_1 s_2 s_2^*$	$s_2 s_1 s_1^*$	$s_3 s_1 s_1^*$	$3\Delta f$	ACI
3 rd	$s_1 s_3 s_3^*$	$s_2 s_3 s_3^*$	$s_3 s_1 s_1^*$	$3\Delta f$	ACI
3 rd	$s_2 s_2 s_3^*$	$s_1 s_3 s_2^*$	$s_2 s_2 s_1^*$	$3\Delta f$	ACI

III. Mitigation Techniques

A. Predistortion

The functionality of the predistorter is to modify the transmitted signal so as to reduce or eliminate non-linear effects. This can be done in several ways⁵, leading to various classes of equalizers. We now present the most relevant of these classifications below; the interested reader is referred to Ref. 5 for details.

2. Classification of Predistortion Techniques

- *Data and Signal Predistortion:* The predistorter achieves its functionality of inverting the channel either operating on the baseband data symbols (data predistorter) or on the baseband analog signal (signal predistorter).
- *Digital and Analog Predistortion:* This classification is based on the technology used to implement the predistorter: analog techniques provide for signal predistortion while digital implementations are essential for data predistortion
- *Lookup Table and Model based Predistortion:* Based on their architecture, DPD algorithms are commonly classified as model based or look-up table based methods. For each constellation symbol, a transmitted symbol is generated using a pre-determined table in the LUT method¹. This method has been used for single carrier transmissions with non-linearity and memory effects¹. On the other hand, a model of the nonlinear dynamic transfer function of the HPA is derived and the pre-distorter is obtained as an inverse of this characteristic in model based mechanisms. The Volterra series described earlier is widely used to describe the non-linearity as well as inverse^{5,10}.

3. Algorithms for Predistortion

Several algorithms for predistortion have been considered in literature for single carrier case^{1, 3, 11, 12, 13}. To adapt some of these methods to multiple carrier scenarios, we restrict ourselves to model based digital predistortion. Data predistortion modifies the constellation symbols before the pulse shaping filter and does not cause out of band interference on the uplink. Moreover, the digital techniques are easy to implement and adapt. On the other hand, LUT¹ is not feasible in multiple carrier scenarios due to the increased number of entries on account of ACI.

A nonlinear dynamic system with memory can be described a Volterra model. Further, its inverse is also a nonlinear dynamic system and can also be described by a Volterra model¹⁰. Thus, a Volterra model is the first choice for a DPD algorithm. However, the Volterra series converges slowly, and in practice various memory polynomials¹³ are used. These are reduced Volterra models and have the advantage that they have fewer coefficients and are faster in convergence. Use of memory polynomials has been considered in a scenario involving two or more RF signals are amplified by the HPA simultaneously^{6,7}. These motivate the use of predistortion based on memory polynomials in this paper and the same is described next.

4. Memory polynomials and their identification

The Volterra series relating the input and output of a non-linear system is given in Eq. (1). A similar model is used at the Volterra DPD where $y(n)$ is now the predistorted symbols while $x(n)$ denote the constellation symbols. Dependence of $y(n)$ on $x(n - k)$, $k > 0$, indicates a nonlinearity with memory (due to IMUX and OMUX) and the predistorter is dynamic in nature⁵. The kernel, $\{h_k(n_1, n_2, \dots, n_k)\}$, is also known as the coefficients of the Volterra DPD. Motivated by this, a third order memory polynomial multicarrier DPD algorithm without ACI (cross talk) relates the pre-distorted signal $u_k(n)$ on the k^{th} channel to the input according to

$$u_k(n) = \sum_{m=0}^{P_{1,k}-1} h_k^{(1)}(m) s_k(n-m) + \sum_{k=1}^M \sum_{m=0}^{P_{3,k}-1} h_k^{(3)}(m) s_k(n-m) |s_k(n-m)|^2 \quad (4)$$

Here, $h_k^{(m)}$ denotes the model coefficients of order m and s_k denotes the symbol on k^{th} carrier. $P_{l,k}$ denotes the memory depth of the order l and channel k . It is clear that the number of co-efficients, are much lower than that in Eq. (1) for a given order leading to the complexity advantage of memory polynomials.

If cross talk is included, the third order memory polynomial predistorter takes the general form,

$$u_p(n) = \sum_{k=1}^M \sum_{m=0}^{P_{1,k}-1} h_{p,k}^{(1)}(m) s_k(n-m) + \sum_{k_1=1}^M \sum_{k_2=k_1}^M \sum_{k_3=1}^M \sum_{m=0}^{P_{3,k_1,k_2,k_3}-1} h_{p,k_1,k_2,k_3}^{(3)}(m) s_{k_1}(n-m) s_{k_2}(n-m) s_{k_3}(n-m)^* + \dots \quad (5)$$

Apart from $h_{p,k}^{(1)}$, additional co-efficients indicating ACI also appear in the form of $h_{p,k_1,k_2,k_3}^{(3)}(m)$. Again, the reduction of co-efficients with respect to Volterra can be observed. It should be noted that symbols on all carriers are used to generate the pre-distorted signal of a particular carrier.

Central to DPD is the identification of necessary coefficients. While direct and indirect learning methods are used in identification, we focus on the indirect learning method. This stems from the fact that indirect learning method is easy to implement and it does not require any real time feedback¹³. The indirect learning method is based on the fundamental pth order theorem that states that the post inverse and pre inverse of a nonlinear dynamic system are identical and that the nonlinear order (p) of the system's inverse is the same as the nonlinear order of the system itself¹⁰. In this method, the coefficients in the algorithm for the inverse of the nonlinear system are identified in a first step using an estimation of the predistorter output error, and in a second step copied to the predistorter function itself. When the input and output in Eq. (4) or (5) are known, the model co-efficients satisfy a linear relation and its form for three carriers is given in Eq. (6) below.

$$\begin{bmatrix} \mathbf{u}_1 \\ \mathbf{u}_2 \\ \mathbf{u}_3 \end{bmatrix} = \begin{bmatrix} \mathbf{H}_1(x) & \mathbf{0} & \mathbf{0} \\ \mathbf{0} & \mathbf{H}_2(x) & \mathbf{0} \\ \mathbf{0} & \mathbf{0} & \mathbf{H}_3(x) \end{bmatrix} \begin{bmatrix} \boldsymbol{\theta}_1 \\ \boldsymbol{\theta}_2 \\ \boldsymbol{\theta}_3 \end{bmatrix} \quad (6)$$

Here, $\mathbf{u}_i = [u_i(1), u_i(2), \dots, u_i(N)]^T$, is the set of received symbols, $\boldsymbol{\theta}_i = [h_1^{(1)}(0), h_1^{(1)}(1), \dots, h_2^{(1)}(P_{1,1} - 1), h_2^{(1)}(0), \dots, h_2^{(1)}(P_{1,2} - 1), h_3^{(1)}(1), \dots, h_3^{(1)}(P_{1,3} - 1), h_{1,1,1}^{(3)}(0), \dots, h_{1,1,2}^{(3)}(0), \dots, h_{1,1,2}^{(3)}(0), \dots, h_{3,3,3}^{(3)}(0), \dots]^T$ denotes all the model coefficients stacked into a vector, $\mathbf{H}_i(x)$ is the regression matrix that describes previous equation and T represents the transposition operator. Clearly, Eq.(6) allows for use of linear methods to identify the coefficients.

B. Equalization

1. Motivation

While multicarrier digital predistortion is implemented at the transmitter side, in reality, it cannot fully compensate the non-linear effects of the channel. The limited model degree and memory as well as the not-invertible nature of the HPA function, do not allow perfect compensation. Hence, without particular assumptions, the resulting channel still possesses the characteristics of a non-linear dynamic system. Hence, non-linear equalization is also considered as a possible enhanced receiver technique. Non-linear equalization would compensate for the residual non linearity and interferences. Further, the system scenarios mandate single carrier equalization where transmissions from other carriers are merely considered as interference.

2. Non-linear equalizers

Equalization is performed on the symbol level after the pulse-shaping filter. Since the cascade of the DPD and the satellite channel is still non-linear due to incomplete compensation, it can be modelled using the Volterra series. Hence, similar to DPD, Volterra equalizers are widely used in satellite literature^{3,4,5}. The equalized output of any carrier, denoted by $y(n)$, is obtained from its input $x(n-k)$, $k \geq 0$, using the following equation

$$y[n] = \sum_{k_1=0}^{K-1} h_1[k_1]x[n-k_1] + \sum_{k_1=0}^{K-1} \sum_{k_2=0}^{K-1} \sum_{k_3=0}^{K-1} h_3[k_1, k_2, k_3]x[n-k_1]x[n-k_2]x[n-k_3]^* + \dots \quad (7)$$

where the $h_*[*]$ are the channel/ Volterra coefficients. Since single carrier equalization is used, $x(n-k)$ is the signal on the desired carrier and that the adjacent channel information is not used.

As mentioned earlier, memory polynomials and their orthogonal version, have found wide application as DPD mechanisms in terrestrial systems. Due to the exponential growth of complexity in Volterra equalizers with increase

in degree, we also consider memory polynomials. Based on Eq. (7), the memory polynomial function is takes the form

$$y[n] = \sum_{k_1=0}^{K-1} h_1[k_1]x[n-k_1] + \sum_{k_3=0}^{K-1} h_3[k_3]x[n-k_3]x[n-k_3]x[n-k_3]^* + \dots \quad (8)$$

Clearly, instead of coefficients $h_3[k_1, k_2, k_3]$ in the Volterra, we only have $h_3[k_1]$ and hence its complexity grows linearly with degree.

In many applications, numerical issues become important in addition to limited computational complexity. The accuracy in estimating the equalizer parameters needs to be optimized and the complexity needs to be reduced. Orthogonal polynomials represent a tailoring of memory polynomials, in which the bases functions are defined to improve numerical stability and accuracy¹⁵. *Orthogonality* usually guarantees these aspects and bases functions are defined to ensure orthogonality in the statistical sense among different degree terms. In particular, the equalizer takes the form in equation (8), where $\psi_*(\cdot)$ denote the bases functions:

$$y[n] = \sum_{k_1=0}^{K-1} h_1[k_1]\psi_1(x[n-k_1]) + \sum_{k_3=0}^{K-1} h_3[k_3]\psi_3(x[n-k_3]) + \dots \quad (9)$$

Further, ψ_i are defined assuming a known input distribution of the variable x such that:

$$E[\psi_k(x)\psi_l(x)^*] = 0 \quad \forall k \neq l \quad (10)$$

In this work, we choose the bases functions derived in Ref. 15. Since orthogonal memory polynomials have the same property and complexity characteristics of memory polynomials, they will also be considered for single carrier equalization.

3. Identification

For a given order and memory, estimation of the kernel co-efficients can be formulated as a Linear Least Squares problem. In this paper, a standard Recursive Least Squares implementation is considered to reduce the complexity and to be able to track channel changes^{8,9}. In all equalization cases, RLS technique is employed to iteratively adapt the kernel coefficients to channel changes according to the following set of equations:

$$u(i) = \begin{bmatrix} x(i) \\ x(i-1) \\ \vdots \\ x(i)x(i)x(i) \\ x(i-1)x(i-1)x(i-1) \\ \vdots \end{bmatrix}$$

$$e(i) = d(i) - u(i)^T h(i-1)$$

$$g(i) = \frac{P(i-1)u(i)^*}{\gamma + u(i)^T P(i-1)u(i)^*}$$

$$P(i) = \gamma^{-1}P(i-1) - g(i)u(i)^T \gamma^{-1}P(i-1)$$

$$h(i) = h(i-1) + e(i)g(i)$$

where $u(i)$ is the vector of all the linear and non-linear terms included by the equalization function (number of terms and form depend on the type of model, degree and memory depth), $h(i) = [h_1^i(0), \dots, h_1^i(K-1), h_3^i(0), \dots, h_3^i(K-1)]^T$, is the vector consisting of the kernel coefficients during the i^{th} instance, $d(i)$ is the desired symbol and γ the forgetting factor.

For all the consider equalization techniques identification is based on training symbols. Each frame is assumed to have a dedicated code_seg¹ of 90 training symbols in the target modulation. This allows supporting Adaptive Code Modulation operation mode foreseen by the standard, as well as channel parameters' drift. From simulation results the forgetting factor has been set to 0.995.

IV. Performance Analysis of Mitigation Techniques

A. Simulation Set-up

The simulation set-up is illustrated in Figure 5 and the simulation parameters are summarized in Table 1. Simulations were performed by choosing the representative case of three carriers, each of 8 MHz (excluding raised cosine bandwidth excess) with the separation between their centre frequencies being 10 MHz. These carriers use a square root raised cosine pulse shaping with an excess bandwidth of 2MHz (roll-off of 0.25). As a result, the adjacent channels are close to each other without any channel spacing. In order to correctly represent the signal at the output of the HPA, a simulation frequency seven times the IMUX bandwidth was used. This accounts the spectral regrowth corresponding to a non-linear order of seventh degree.

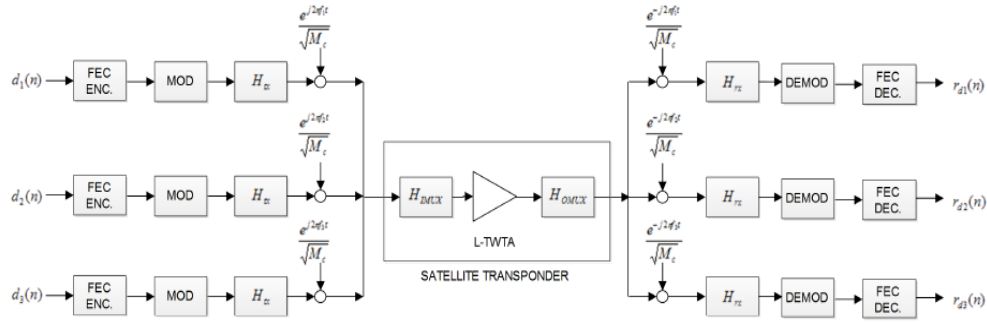


Figure 5: Schematic diagram of the simulation chain

Table 2: Simulation Parameters

System	Number of carriers	3
	Symbol Rate	8 Mbaud
	Carrier Frequency Spacing	1.25 *Rs
	Modulation	32 - 16 - 32 APSK
	Code Rate	$\frac{3}{4}$ - $\frac{2}{3}$ - $\frac{3}{4}$
	Roll-off factor (all carriers)	0.25
Channel	IMUX pass-band (3 dB)	29 MHz
	OMUX pass-band (3 dB)	30 MHz
	HPA type / model	Linearized Ku-band / Saleh
	Es/N0 (dB)	12 - 9 -12

Noise power, chosen according to Es/N0, is added at the output of OMUX. This stems from the fact that noise power at the receiver is fixed. Hence, the actual SNR at the receiver is not constant, but varies with the signal power as dictated by the operating point of HPA.

1. Channel Models

The well-known Saleh model⁵ is used to model HPA. Such model is defined by :

$$F_a(|x(n)|) = \frac{a_0|x(n)|}{1 + a_1|x(n)|^2}, \quad F_p(|x(n)|) = \frac{b_0|x(n)|^2}{1 + b_1|x(n)|^2} \quad (11)$$

Here $F_a(|x(n)|)$, $|$ denotes the AM/ AM distortion while $F_p(|x(n)|)$ denotes the phase distortion (AM/PM distortion). With the input to the HPA being $x(n) = |x(n)|e^{j\theta}$, the output takes the form, $y(n) = F_a(|x(n)|)e^{j(\theta + P_p(|x(n)|))}$

The IMUX and OMUX filters are modelled as FIR functions. The straightforward implementation of the FIR filter model is directly in the up-sampled simulation frequency domain. Thus the sampling frequency of the FIR will correspond to the simulation frequency F_s . Sampling frequency and number of taps control both accuracy and complexity. The FIR filter coefficients ($h(t_k)$, $k = 0, \dots, M - 1$) are obtained from frequency domain measurements ($H(f_k)$, $k = 0, \dots, N - 1$) using the well-known over-determined (or averaged) Frequency sampling method. In this method, the coefficients are obtained as the LS solution of the following overdetermined ($N > M$) set of equations:

$$\begin{bmatrix} H(f_0) \\ \vdots \\ H(f_{N-1}) \end{bmatrix} = \begin{bmatrix} e^{-j2\pi f_0 t_0} & \dots & e^{-j2\pi f_0 t_{M-1}} \\ \vdots & \ddots & \vdots \\ e^{-j2\pi f_{N-1} t_0} & \dots & e^{-j2\pi f_{N-1} t_{M-1}} \end{bmatrix} \begin{bmatrix} h(t_0) \\ \vdots \\ h(t_{M-1}) \end{bmatrix} \quad (12)$$

The obtained FIR will be the optimum in the minimum squared sense with respect to the provided measurements.

A. Performance

1. Figure of Merit

The widely used FoM to characterize performance on the nonlinear satellite channels is the total degradation defined as

$$TD = \left. \frac{E_b}{N_0} \right|_{NL} - \left. \frac{E_b}{N_0} \right|_{Ideal} + OBO. \quad (13)$$

The term $\left. \frac{E_b}{N_0} \right|_{NL} - \left. \frac{E_b}{N_0} \right|_{Ideal}$ reflects the loss in SNR of a practical HPA compared to ideal HPA for achieving the same BER at the same OBO levels. This term is penalized by OBO to reflect on the loss in power efficiency with high OBO. As OBO increases, the practical HPA is pushed more and more into the linear region and $\left. \frac{E_b}{N_0} \right|_{NL} - \left. \frac{E_b}{N_0} \right|_{Ideal}$ reduces. Thus one could see a trade-off between the two components and an optimum OBO minimizing the TD is usually seen.

Evaluating the TD in the framework of DVB-S2 requires implementation of the LDPC and the ensuing simulations are time consuming (as it involves Decoding of LDPC codes). Since the entire chain is not simulated currently, we use SINR as an alternative metric since i

1. Shows a behaviour consistent with TD
2. Faster to compute since it works on uncoded systems

To reflect on the similarities between TD and SINR, we see that the OBO affects the SINR as follows:

- Low OBO leads to high interference (non-linear region) but higher SNR (higher amplification of the signal)
- High OBO leads to low interference (linear region) but low SNR (lower amplification)

This defines an optimum OBO where SINR shows its maximum. This maximum represents the compromise between noise and interference.

When the transmitted symbol $s(n)$ is received as $y(n)$ after appropriate processing (DPD->IMUX->HPA->OMUX->EQ), the SINR is evaluated as

$$\rho = \frac{E[|s(n)|^2]}{E[|y(n) - s(n)|^2]} \quad (14)$$

In Eq. 14, we assume, without loss of generality, that the resulting path gain on the signal of interest is unity. In practice, DPD/ EQ design strives to ensure that the received signal has a unity gain for the useful component and the aforementioned signal model is deemed appropriate. Finally scaling of the received signal does not alter the SINR.

2. Predistortion only Scenario

As preliminary analysis we consider the case in which only predistortion is applied and so no equalization is performed at the receivers' side. Multicarrier DPD with and without cross-terms as it is described in section III is hereafter considered. Notice that DPD without cross-terms basically corresponds to standard single carrier DPD applied separately to each channel (this latter version in the figures is labelled NC that stands for No Cross-terms included).

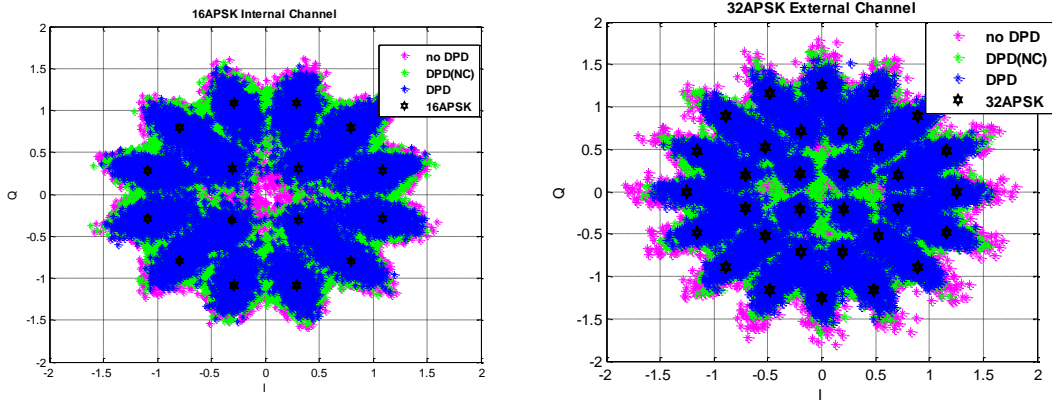


Figure 6: Channel output scatter plots for different DPD, Noise less case

In Figure 6, we see the noiseless scatter plots of the received symbols for the external and internal channels, respectively. The scatter plots give an idea on how the clustering and warping effects are reduced by the applied techniques. In particular we can see how DPD improves the shape of received samples compared to the cases in which DPD is not including cross terms or is not applied at all.

In Fig. 7 we see the SNIR performance, when only predistortion is applied, for the channel configuration of Table 2.

Observing Fig. 7 we notice that, for the internal carrier, the application of predistortion not including cross terms actually degrades the performance. In the internal channel memory effects are negligible and ACI are dominant. Therefore applying a predistortion function that does not include cross terms brings to a model mismatch. On the other hand, in the external channel, where the dominant impairments are related to ISI, we have a significant gain between the two techniques. In fact the external channels, positioned on the filter bandwidth's edge, suffer of significant memory effects leading to strong linear and non-linear ISI. On the other hand they experience lower ACI being external in frequency.

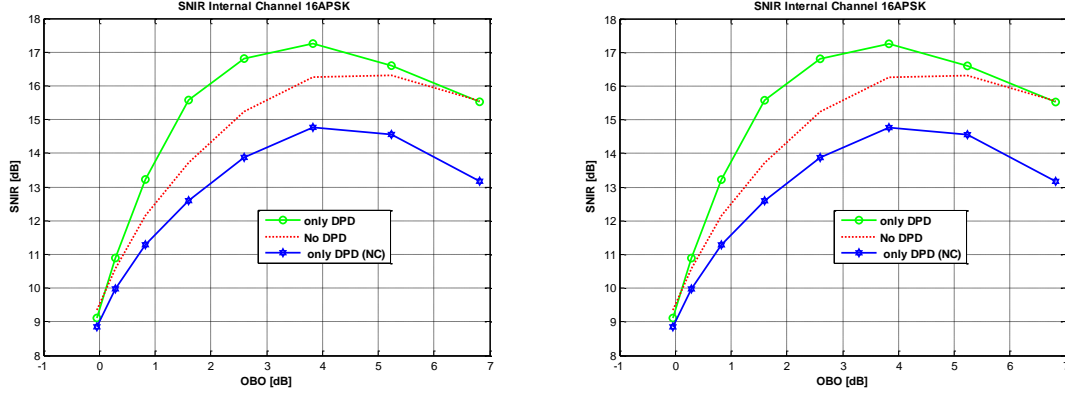


Figure 7: SNIR of Predistortion only applied: Internal Channel (left) and External Channel (right)

3. Equalization only Scenario

As a further step in the analysis, we now consider the situation where only equalization is applied. Recall that we implement a single carrier equalizer that is capable of compensating both linear and non-linear ISI while it fails to cancel ACI since it does not process symbols of the other carriers (unlike multicarrier equalization in Ref. 8-9). Some results of the equalization only approach with channel configuration of Table 2 are presented below.

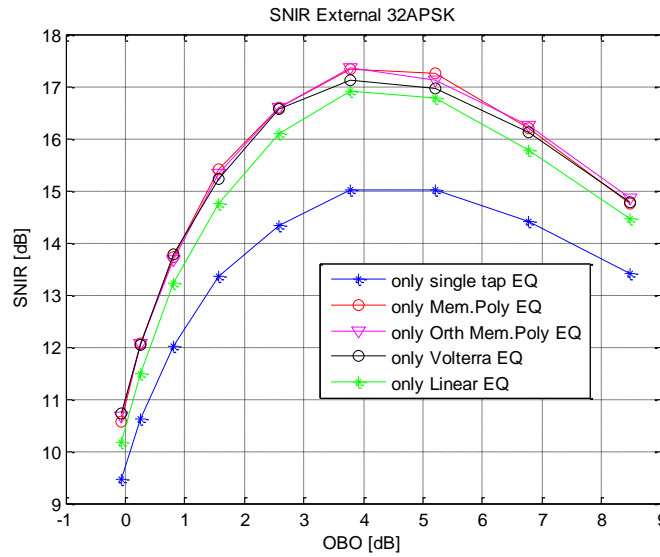


Figure 8: SINR for different Equalizers: External Channel

Figure 8 shows the significant gain between the solution without equalization (a single tap filter compensating only warping) and other architectures for the external channel (the two external channels have similar behaviour and only one is reproduced). This is related to the presence of strong linear ISI coming from the filtering effects present at the edge of the transponder bandwidth. The relative gain between linear and non-linear equalization techniques is instead limited since both non-linear ISI and ACI are, rather, negligible compared to linear ISI effects. On the other hand, as depicted in Figure 9, memory effects (ISI) are negligible for the internal carrier and a significant SNIR gain is achieved by non-linear equalization. Further SINR improvement in this case cannot be achieved because ACI cannot be effectively cancelled with single carrier equalization. This justifies the definition of multicarrier (joint) DPD at the GW to in order to pre-compensate at best ACI

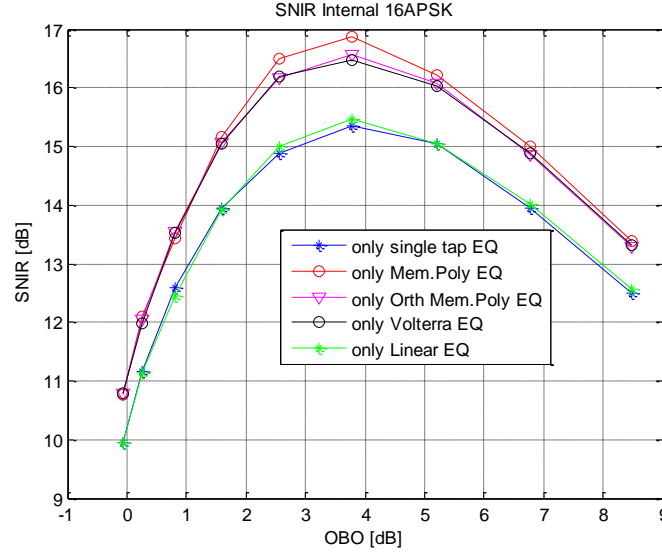


Figure 9: SNIR for different Equalizers: Central Channel

Comparing the only predistortion approach with the only equalization one, we can notice a major degradation in the internal channel in the only equalization case. The internal channel suffers predominantly from ACI and single carrier equalization cannot effectively compensate for that. On the other hand, DPD with cross terms has the wherewithal to cancel ACI.

4. Combined Predistortion and Equalization

In the following we illustrate the consolidate gain of the mitigation techniques in which we combine predistortion and equalization together in order to achieve the best performance.

In the external channel multicarrier predistortion is fairly effective in compensating both ISI and ACI and so no additional gain is achievable with single carrier equalization techniques. This is clearly seen from Fig. 10. Single carrier predistortion (no cross terms) provides significant gain compensating for linear and non-linear ISI. As already highlighted in the only predistortion case (Fig. 9), on the internal channel, being ACI the dominant impairment, the solution applying DPD without cross terms produces a modelling mismatch resulting in performance degradation (kindly refer to Fig. 11). With multicarrier DPD (cross-terms included), we have instead a significant SINR gain, especially in the saturation region. However, differently from the external channel case, some residual memory effects and non-linear interferences are still present in the signal and equalization provides some further improvement in SINR.

In this combined DPD and EQ case of study, Orthogonal polynomials and Volterra equalization, in conjunction with multicarrier DPD, seem to provide the best performance in the optimum OBO region. In the region close to saturation all the non-linear equalization techniques have similar performance gains. These representative results show the SINR improvement in using non-linear mitigation techniques at either end, as compared to situation without DPD and EQ. This gain is available not only at the optimum OBO, but also closer to saturation. Although maximum SNIR would represent the maximum capacity region with respect to OBO, we are also interested in the SINR gain closer to the saturation region where power efficiency is higher. In this region, coding techniques could be applied in order to achieve the optimum compromise between throughput and power efficiency. The plots also corroborate the fact that non-linear equalizers can give gains, both with and without the use of DPD.

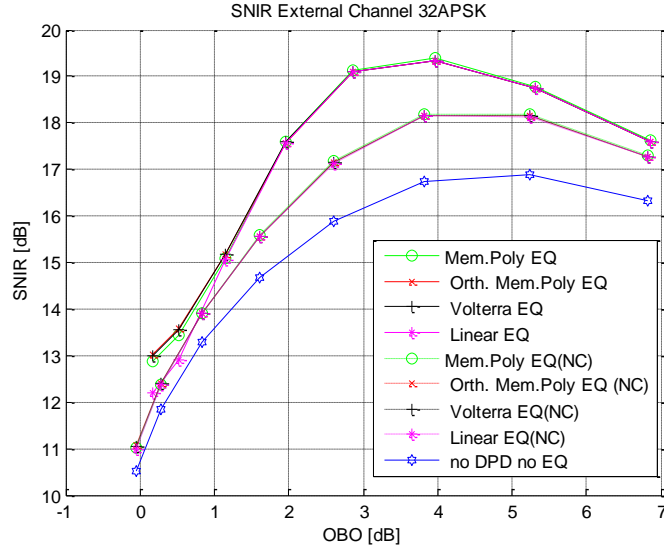


Figure 10: SINR of Combined Predistortion and Equalization Techniques: External Channel

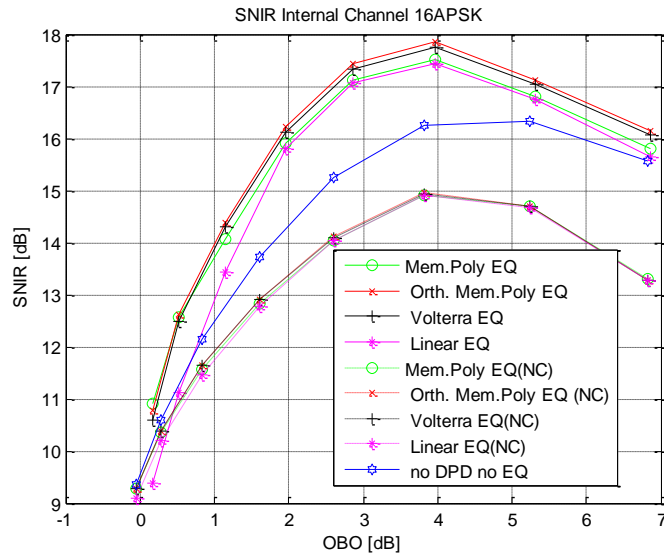


Figure 11: SINR of Combined Predistortion and Equalization Techniques: Central Channel

V. Conclusions

The paper studied the use of non-linear mitigation techniques to the situation where multiple carriers were amplified by a single HPA. The transmitter processing (predistortion) is privy to the data on the multiple carriers while the receive processing (equalization) has only access to desired carrier. Several algorithms are considered and the use of processing at either end shows significant SINR gain at low OBO region (2-3 dB). This SINR gain can be exploited by coding techniques to further reduce the OBO and improve power efficiency. A final confirmation of this is awaited, pending Total Degradation and overall system efficiency evaluations, to assess the achievable gain with respect to actual benchmark for multicarrier systems. The study also provides a first understanding of the gains obtained by use of predistortion only/ equalization only and can be useful in system design.

Acknowledgments

This work is supported by the ESA Contract. No. 4000105192/12/NL/AD, “On Ground Multicarrier Digital Equalization/Predistortion Techniques for Single or Multi Gateway Applications”.

References

- ¹ Casini. E, De Gaudenzi. R and Ginesi. A, “DVB-S2 modem algorithms design and performance over typical satellite channels,” *International Journal of Satellite Communications and Networking*, Vol. 22, 2004, pp. 281–318.
- ² ETSI EN 302 307 V1.2.1 (2009-08), “Digital Video Broadcasting (DVB); Second generation framing structure, channel coding and modulation systems for Broadcasting, Interactive Services, News Gathering and other broadband satellite applications (DVB-S2)”
- ³ Giugno. L, Luise. M and Lottici. V, “Adaptive Pre and Post-Compensation of Nonlinear Distortions for High-Level Data Modulations,” *IEEE Transactions on Wireless Communications*, Vol. 3, No. 5, 2004, pp. 1490-1495.
- ⁴ Benedetto. S and Biglieri. E, “Nonlinear equalization of digital satellite channels,” *IEEE Journal on Selected Areas in Communications*, Vol. 1, Jan. 1983, pp. 57-62
- ⁵ Corazza. G. E, *Digital Satellite Communications*, Chapter 8, Springer, 2007.
- ⁶ Bassam. S. A, Helaoui. M, and Ghannouchi. F. M, “Crossover Digital Predistorter for the Compensation of Crosstalk and Nonlinearity in MIMO Transmitters,” *IEEE Transactions on Microwave Theory and Techniques*, Vol. 57, No. 5, 2009, pp. 1119-1128.
- ⁷ Bassam. S. A, Chen. W, Helaoui. M, Ghannouchi. F. M, and, Feng. Z, “Linearization of Concurrent Dual-Band Power Amplifier Based on 2D-DPD Technique,” *IEEE Microwave and Wireless Components Letters*, Vol. 21, No 12, Art. no. 6051495, 2011, pp. 685-687.
- ⁸ Beidas. B and Seshadri. R, “Analysis and Compensation for Nonlinear Interference of Two High-Order Modulation Carriers over Satellite Link” *IEEE Transactions on Communications*, Vol. 58, No. 6, June 2010
- ⁹ B. F. Beidas, “Intermodulation Distortion in Multicarrier Satellite Systems: Analysis and Turbo Volterra Equalization,” *IEEE Transactions on Communications*. Vol. 59, No. 6, June 2011, pp. 1580-1590.
- ¹⁰ Schetzen. M, *The Volterra and Wiener theories of nonlinear systems*, Wiley, New York, 1989.
- ¹¹ Isaksson. M and Rönnow. D, “A parameter-reduced volterra model for dynamic RF power amplifier modeling based on orthonormal basis functions,” *International Journal of RF and Microwave Computer-Aided Engineering*, Vol. 17, No 6, 2007, pp. 542-551.
- ¹² Gilabert. P. L, Montoro, G, Bertran. E, “On the Wiener and Hammerstein Predistortion,” *Proceedings of APMC*, Vol. 2, 2005, pp. 1191-1194.
- ¹³ Ding. G, Zhou. G. T, Morgan. D. R, Ma. Z., Kenney. J. S, Kim and J, Giardina. C, R “A robust digital baseband predistorter constructed using memory polynomial,” *IEEE Transactions on Communications*, Vol. 52, No. 1, 2004, pp. 159-165.
- ¹⁴ Colavolpe. G and Piemontese. A, “Novel SISO Detection Algorithms for Nonlinear Satellite Channels” *Proceedings of IEEE Global Telecommunications Conference*, Jan. 2011, pp. 1-5.
- ¹⁵ Raich. R, Hua. Q and Zhou, G. T, “Orthogonal polynomials for power amplifier modelling and predistorter design,” *IEEE Transactions on Vehicular Technology*, Vol. 53, No 5, 2004.